Probing the f electrons in URu_2Si_2 with positrons: A theoretical investigation

G. J. Rozing and P. E. Mijnarends
Netherlands Energy Research Foundation ECN, 1755 ZG Petten, The Netherlands

D. D. Koelling
Materials Science Division, Argonne National Laboratory, Argonne, Illinois 60439
(Received 11 July 1990; revised manuscript received 25 October 1990)

The two-photon momentum distribution for positron annihilation is computed for the heavy-fermion system URu_2Si_2. A nonrelativistic approximation of the positron-electron overlap integrals is applied to wave functions obtained from a fully relativistic, self-consistent band-structure calculation. The crystal structure causes a preference of the positron for the uranium site, resulting in a considerable contribution to the two-photon momentum distribution of the f-electron states and marked structure related to the Fermi surface. Results are presented for integration of the two-photon momentum distribution along the [001] and [101] directions. Subsequent application of the Lock-Crisp-West theorem reveals Fermi-surface effects superimposed on long-wavelength structure due to the inhomogeneity of the positron wave function. It is concluded that positron annihilation can be used to study the nature of the f electrons in this heavy-fermion system.

I. INTRODUCTION

Measurements of the two-dimensional angular correlation of annihilation radiation (2D-ACAR) on single crystals provide the once-integrated two-photon (2γ) momentum distribution.[1] Since the 2γ momentum distribution displays discontinuities caused by the Fermi surface (FS) and its shape reflects the wave-function symmetry of the occupied electron states,[2] 2D-ACAR experiments can provide direct experimental information about the electronic structure of a solid on the same microscopic level as de Haas–van Alphen experiments. However, in order to obtain experimentally detectable effects, a significant wave-function overlap between the positron and the electrons is required. In this paper we employ a recently developed relativistic formalism[3,4] to calculate the 2γ momentum distribution for the heavy-fermion system URu_2Si_2.

Heavy-fermion systems are compounds, usually containing Ce and U, with strongly renormalized electron masses. The measured electronic specific-heat coefficient of URu_2Si_2 in the antiferromagnetically ordered state is[5,6] 65 mJ/mol K^2. Although the lower bound for heavy-fermion behavior was arbitrarily chosen[7] to be 400 mJ/mol K^2, the compound URu_2Si_2 can be considered to be characteristic for a heavy-fermion system. But what really attracted the attention of the solid-state community was the discovery of magnetic order and superconductivity coexisting below 1 K by Broholm *et al.*[8] Similar results obtained by Aeppli *et al.*[9] for another heavy-fermion superconductor, UPt_3, suggest that the magnetic order may be essential for this new type of superconductivity.

Recently, we have performed 2D-ACAR measurements on single crystals of URu_2Si_2. Results of these measurements and a comparison with the present calculations will be presented elsewhere. The purpose of this paper will be to establish the applicability of the positron-annihilation technique to study the nature of the f electrons in this heavy-fermion system.

II. CALCULATIONAL DETAILS

The crystal structure and Brillouin zone of URu_2Si_2 are shown in Fig. 1. The crystal structure is body-centered tetragonal with point group $I4/mmm$ ($ThCr_2Si_2$ type), which is a moderately open structure leaving a large volume for the uranium atom. This works to our advantage since this large interstitial region around the uranium atom helps to pull the positron to it and aids in the sensitivity to the f states.

The energy band structure is calculated by solving the full Dirac equation using the relativistic linearized augmented-plane-wave (RLAPW) method[10] in a quaternion formulation[11] and iterating to self-consistency. The maximum length of the reciprocal-lattice vectors of the RLAPW basis functions is 4.25 a.u. and the angular decomposition of the wave functions inside the spheres includes all angular momenta (j) up to $l=8$. The potential includes Hedin-Lundqvist exchange-correlation.[12] For the self-consistent-field (SCF) process, the Brillouin zone is sampled on a set of 21 inequivalent points. This poor sampling is probably the weakest point of the calculation. The lattice parameters are $a=7.7932$ a.u. and $c=18.0594$ a.u. and the U-Si distance along the [001] direction is $0.3727c$. The "warped" muffin-tin shape approximation (which spherically averages the potential in the vicinity of the atoms, but retains the full structure of the potential in the interstitial region, the critical area for the positron) is utilized with muffin-tin radii of 3.220, 2.643, and 1.800 a.u. for the U, Ru, and Si spheres, respectively. In the interstitial region (37% of the unit-cell volume) 720 stars of plane waves represent the potential. During the SCF iterations a soft-core treatment[13] proper-

ly takes into account the tails of the core charges which extend into the interstitial region. The final band-structure results are obtained for 671 wave vectors in a $\frac{1}{16}$ irreducible wedge of the Brillouin zone, which yields 11 points along both ΓZ and ΓX (i.e., the $\langle 001 \rangle$ and $\langle 110 \rangle$ directions), respectively.

The 2γ momentum distribution $\rho_{2\gamma}(\mathbf{p})$ is calculated in the independent-particle model using the method described by us elsewhere.[4] This method employs a nonrelativistic approximation for the overlap integral

$$\rho_{2\gamma}(\mathbf{p})=\sum_{\mathbf{k},n} f_n(\mathbf{k}) \left| \int e^{-i\mathbf{p}\cdot\mathbf{r}} \psi_+^\dagger(\mathbf{r}) \gamma_5 \psi_n(\mathbf{k},\mathbf{r}) d\mathbf{r} \right|^2 , \quad (1)$$

where $\psi_n(\mathbf{k},\mathbf{r})$ and $\psi_+(\mathbf{r})$ are the fully relativistic (four-component) wave functions of the electron state with wave vector $\mathbf{k}$ and band index n and the thermalized positron in its ground state at $k_+=0$, respectively. Owing to the coupling matrix

$$\gamma_5 = - \begin{bmatrix} 0 & 1 \\ 1 & 0 \end{bmatrix} ,$$

the overlap integral equals the sum of the product of the large electron and positron components and the product of their small components, respectively. The occupation of the electron states is determined by the Fermi-Dirac distribution function $f_n(\mathbf{k})$. To facilitate the computation of the overlap integral, two approximations are made to the positron wave function. In general, the positron wave function is almost spherically symmetric inside the muffin-tin spheres; therefore, only the $l=0$ term in the angular decomposition is retained. Secondly, since the positron predominantly occupies the interstitial region where the potential is weak, it is valid to neglect the small components of the positron wave function. Consequently, only the product of the large components is included in the calculation of the overlap integral.

The positron wave function is calculated using the self-consistent electron potential after subtraction of the exchange-correlation term and sign reversal. The RLAPW expansion for the positron wave function in URu_2Si_2 is well converged at a reciprocal-lattice-vector length of 2.0 a.u. In the angular decomposition inside the spheres, terms with $l>0$ are found to contribute less than 1% to the charge in each sphere. In Fig. 2 the positron density in the unit cell is plotted. The U sphere contains 30.1% of the positron charge, the Ru spheres each 11.1%, and the Si spheres, 1.3%. The interstitial region, left with 46.1% of the positron charge, attains maximum positron density between neighboring U atoms in the (001) plane. The high positron density found in the vicinity of the U sites is further illustrated in Fig. 3. This figure shows that the positron wave function by its large amplitude inside the U sphere efficiently samples the tails of the f-electron states, thus compensating for the localized character of the f states.[14] The absence of higher l terms in the positron wave function in the U sphere is rather striking considering the anisotropic behavior just

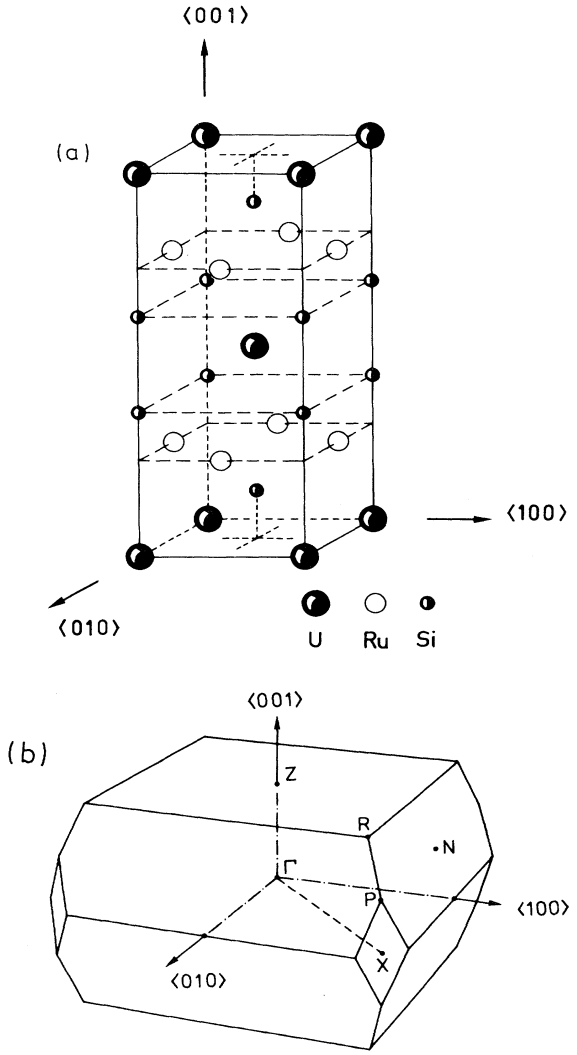

FIG. 1. (a) Crystal structure and (b) Brillouin zone of body-centered tetragonal URu_2Si_2.

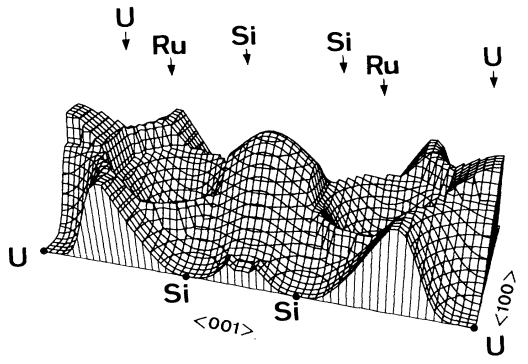

FIG. 2. Positron density in the (010) plane containing the U atoms. Inside the muffin-tin spheres only the $l=0$ terms are included. The position with the largest positron density lies in the middle between two neighboring U atoms, closely followed by the rim around the U atoms. Positron-electron correlation has not been included (cf. Ref. 14).

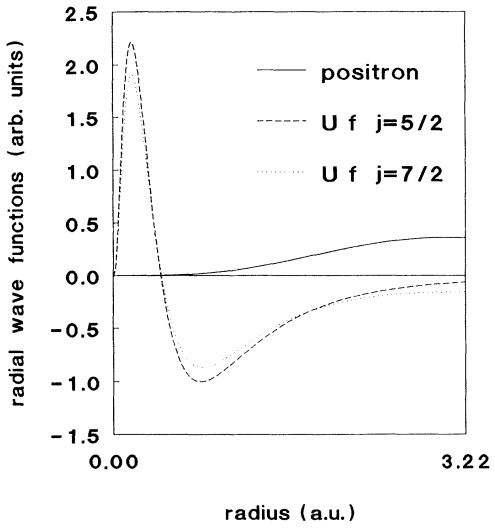

FIG. 3. Radial wave functions (large components) for the positron and the f electrons inside the U muffin-tin sphere. The positron s radial wave function is calculated with $E=-0.08$ Ry. The energy parameters of the f radial wave functions are 0.80 Ry ($j=\frac{5}{2}$) and 0.75 Ry ($j=\frac{7}{2}$), respectively.

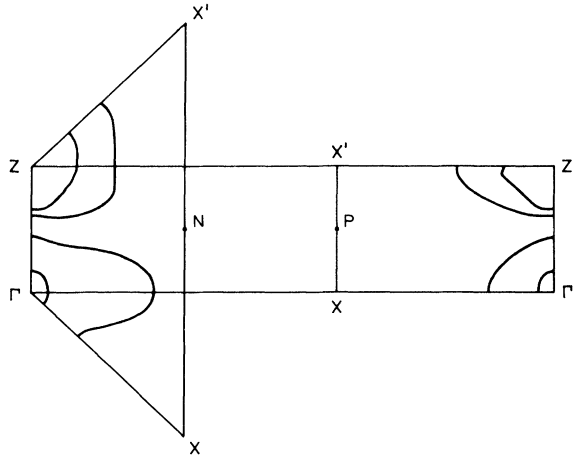

FIG. 5. Calculated Fermi surface of URu_2Si_2. Its intersections with a simplified rectangular Brillouin zone are shown. The symmetry point X' lies in the second zone and is equivalent to point X in the first zone. Owing to the low dispersion of the bands at the Fermi level, the Fermi surface is sensitive to details of the calculation.

outside the sphere, illustrated in Fig. 2. Yet, this fact facilitates the calculation of the 2γ momentum distribution. The 2γ momentum distribution is calculated for 128 000 **p** vectors in the $\frac{1}{16}$ irreducible wedge of **p** space up to $|\mathbf{p}|=3$ a.u. The spacing of the grid equals 0.0403 and 0.0348 a.u. in the [100] and [001] directions, respectively.

III. RESULTS

The calculated electronic band structure of URu_2Si_2 is shown in Fig. 4. The results are similar to previous calculations by Norman *et al.*[15] using the relativistic linear-muffin-tin-orbitals (RLMTO) method. In both calculations a complex of flat energy bands is present near E_F that gives rise to a Fermi surface (shown in Fig. 5), which consists of two concentric electron surfaces centered at Γ and two concentric hole pockets at Z. In addition, the RLMTO calculation yields a complicated sheet originating from the same band that gives rise to the largest hole surface. In the RLAPW calculation this band stays well below E_F, except at point N where it approximates E_F within 2 mRy. This feature might in particular be affected by the limited sampling of the Brillouin zone in the SCF cycles. The angular decomposition of the electron states at the Fermi surface in our RLAPW calculation yields a predominant U f character with some admixture of Ru d and U d symmetry. The wave functions on the hole surfaces show in addition some Ru p character. In Fig. 6 we have plotted the density of states (DOS), along with the U f and Ru d partial DOS. Approximately 2.5 electrons occupy the U f peaks, which have their centers of mass at 0.01 Ry ($j=\frac{5}{2}$) and 0.08 Ry ($j=\frac{7}{2}$) above E_F, respectively. The DOS at E_F amounts to 24 Ry^{-1} per spin per formula unit, but is extremely sensitive to the exact value of E_F.

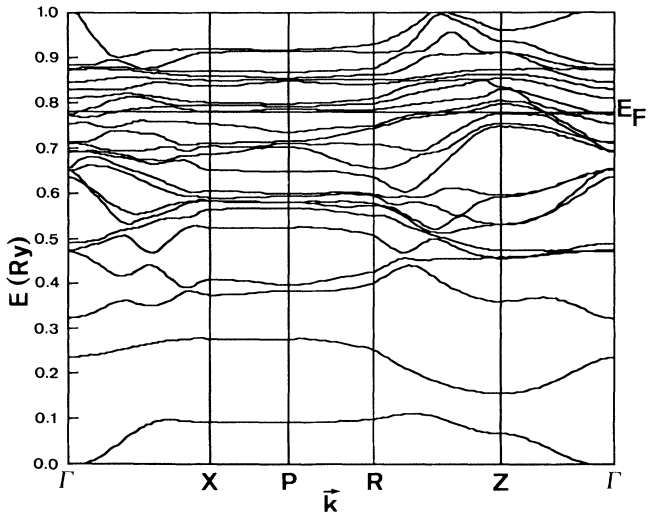

FIG. 4. Energy bands along symmetry lines in the (110) plane in the Brillouin zone.

Figure 7 shows the 2γ momentum distribution in the (100) and (001) planes containing the origin in the form of a contour diagram. Maxima are observed at $p=0.5$ a.u. along the ⟨100⟩ directions. The lowest band shown in Fig. 4 contributes 80% of the total momentum density at $p=0$, owing to the high content of s symmetry, predominantly at the Si sites, of the corresponding wave functions. Its contribution extends to ~1 a.u. in the basal plane and to ~0.5 a.u. along the [001] direction. The second sp-like band, centered at 0.2 Ry, holds no 2γ momentum density in the (001) plane including the ori-

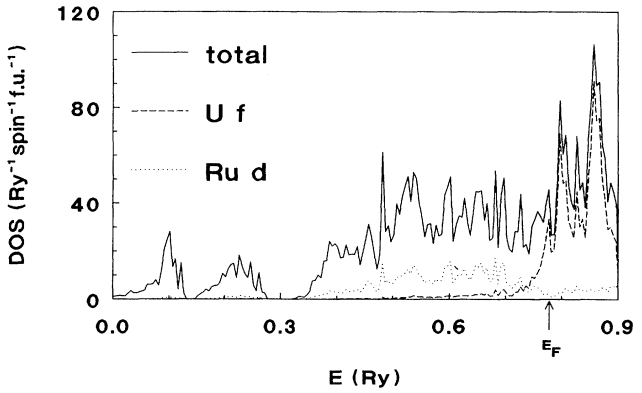

FIG. 6. Density of states in the energy interval from 0.0 to 0.9 Ry. The Fermi energy equals 0.7832 Ry. The dashed curve and the dotted curve show the U f and Ru d projected DOS, respectively. The latter include only the charge inside the muffin-tin spheres and, consequently, the projected DOS cannot be compared directly to the total DOS. The bands between 0.0 and 0.3 Ry contain hybrid states with mainly sp contributions from all spheres.

gin, and contributes predominantly along the [001] direction. Together, the latter two bands yield a momentum distribution which is approximately isotropic. In addition to the bands shown in Fig. 4, the band-structure calculation yields three U $6p$ core states at -0.96 ($j=\frac{1}{2}$), -0.45, and -0.43 Ry (both $j=\frac{3}{2}$), respectively, represented by bands which display hardly any dispersion. The sum of their contributions to the 2γ momentum distribution is quite large with a maximum value of 0.14 at $p=0.6$ a.u. along the $\langle 100 \rangle$ directions. It is noteworthy that, in addition to this relatively large magnitude, the total contribution of these states is weakly anisotropic, unlike the contribution from deep core shells. The bands above 0.75 Ry, involving the hybrid f states, display momentum density at $p > 1.4$ a.u. along the $\langle 100 \rangle$ axes, while only minor contributions are observed along the $\langle 110 \rangle$ axes. Along the [001] axis f-state contributions are found at both small and large momenta, illustrated by the distinct Fermi-surface discontinuities visible in Fig. 7. The marked Fermi-surface structure in the (010) plane, including the [001] axis, is almost exclusively due to the two hole pockets centered at Z. On the other hand, the weak features found in the (001) plane near $p=0.8$ a.u. along the $\langle 110 \rangle$ axes originate in the two electron surfaces at Γ.

To examine the influence of the positron wave function, we have also calculated the 2γ momentum distribution assuming a constant positron density in the unit cell. That is, the upper and lower components of the positron wave function were set equal to 0 and 1 (apart from a normalization constant), respectively. The effect of this, compared to the calculation with the real positron wave function, is a mere reduction of momentum density for small momenta whereas the 2γ momentum distribution at larger momenta is slightly increased. Most importantly, the general shape of the 2γ momentum distribution is not affected, which indicates that the positron wave function does not dominate the 2γ momentum distribution over the electronic-structure effects.

Examination of the Fermi-surface effects in the 2γ momentum distribution is facilitated by the Lock-Crisp-West (LCW) procedure.[1,16] A mapping of the three-dimensional (3D) 2γ momentum distribution in **p** space onto the first Brillouin zone by translation over reciprocal-lattice vectors provides an LCW-folded 2γ momentum distribution, which can be shown to display discontinuities at the Fermi surface, superimposed on a nearly flat background contributed by the completely

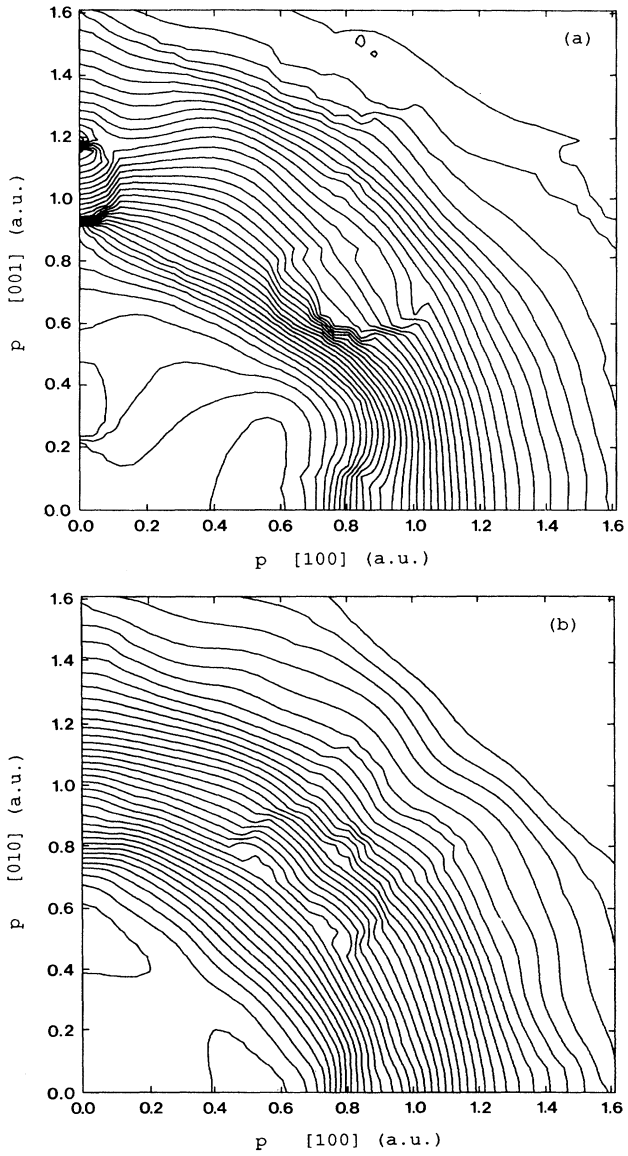

FIG. 7. (a) Contour diagrams of the 2γ momentum distribution in the (010) plane and (b) in the (001) plane. The contour values are separated by 0.02.

filled bands. Additional structure is expected when the positron density is not homogeneously distributed in the unit cell, which we find to be the case in URu_2Si_2, as seen in Fig. 2. Application of the LCW procedure to the 2γ momentum distribution calculated for URu_2Si_2 yields discontinuities with a size of approximately 0.5 for each of the Fermi-surface sheets. This value exceeds the amplitude of the LCW discontinuities caused by the d bands in most transition metals,[17] which is attributed to the crystal structure which allows a large overlap of the positron wave function with the f states. However, this remarkably large value of 0.5 still amounts to only 4% of the background owing to the large number of filled bands. The inhomogeneous distribution of positron charge in the unit cell causes an additional variation in the LCW distribution of approximately 5%. The maxima of this variation lie at Γ, X, and P and the minima at points Z and N.

A 2D-ACAR measurement yields the 2γ momentum distribution integrated along a direction in momentum space specified by the orientation of the monocrystalline sample. In order to predict the size of Fermi-surface-related structure in the actual experiment, the calculated LCW-folded 2γ momentum distribution is integrated along two different directions. As the wave-vector grid is rather coarse, a linear-interpolation procedure is employed to properly take into account the location of the Fermi-surface discontinuities in the integration. Figure 8(a) shows the result for the [001] integration direction in the form of a contour diagram, while Fig. 9(a) shows cuts through the LCW distribution along lines of high symmetry. This two-dimensional LCW distribution is dominated by a principal maximum at the projection of the symmetry points X and P, which results from the positron-electron overlap integrals due to the inhomogeneous positron wave function. Since the Fermi-surface sheets at Γ and Z overlap in projection, a complicated structure appears with an amplitude of the order of 1% of the background, which is very small for observation in a 2D-ACAR experiment. Several integration directions allow the separate observation of the electron and hole surfaces. The [101] direction is found to be least disturbed by the positron wave-function effect. The LCW distribution integrated along the [101] direction is shown in Figs. 8(b) and 9(b). The maximum at ΓN and the minimum at ZN both amount to $\sim 4\%$ of the background and reflect the shapes of the Fermi-surface sheets in projection very clearly. Shifts of the bands which modify the Fermi surface express themselves very clearly in this LCW distribution.

The small components of the electron wave functions

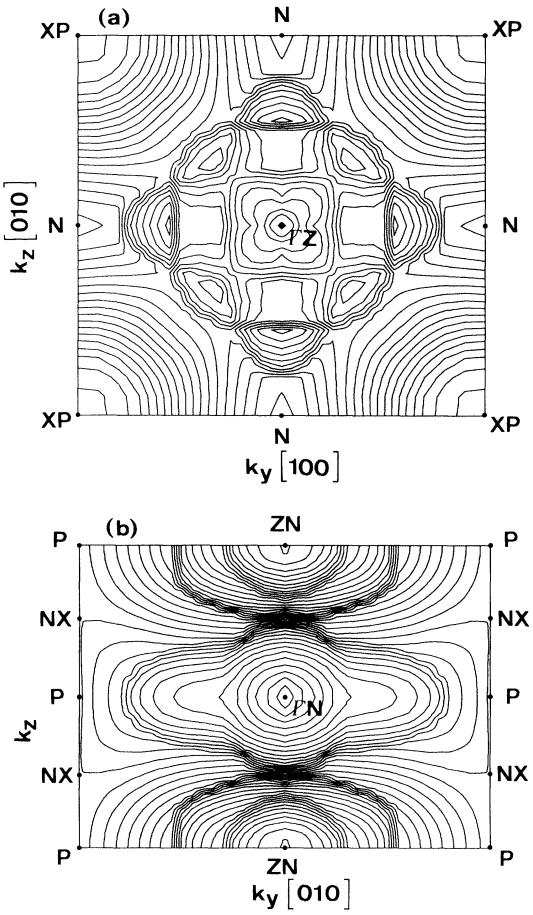

FIG. 8. Contour plots of the LCW distributions calculated for the (a) [001] and (b) [101] integration directions, respectively. Only the LCW unit cell is shown. Contour values are equidistantly distributed between the minimum and maximum. Please remember that the direction [101] lies along the vector $(2\pi/a, 0, 2\pi/c)$. Hence, the k_z axis in (b) does not coincide with a crystallographic symmetry direction.

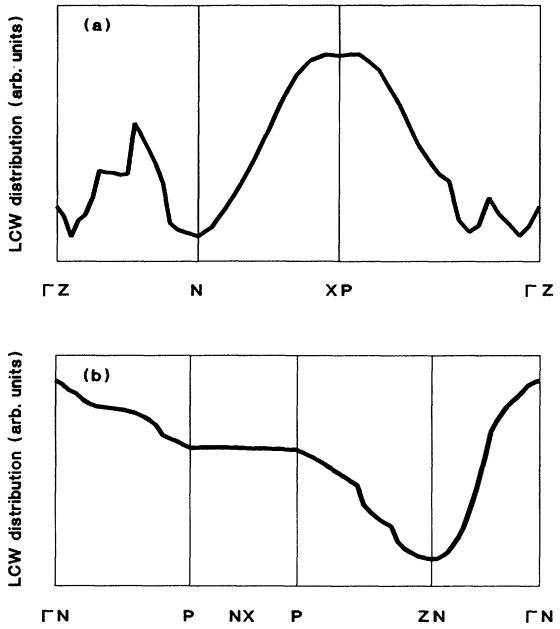

FIG. 9. Cuts along lines of high symmetry through the distributions shown in Fig. 8. Integration along (a) the [001] and (b) the [101] direction.

contribute to the 2γ momentum distribution via the product of small electron and positron components according to the coupling by the γ_5 matrix in Eq. (1). However, since the small positron components can be neglected, this product vanishes and the small electron components affect the 2γ momentum distribution only as a result of the normalization of the electron spinors, which does include the small components. It can be shown[4] that the three-dimensional LCW-folded 2γ momentum distribution at wave vector $\mathbf{k}$ is reduced with respect to the number of occupied bands according to the magnitude of the small electron components of the states at $\mathbf{k}$. From our calculation with the upper (small) and lower (large) positron components set to 0 and 1, respectively, we find that this reduction equals 5% and is uniform throughout the Brillouin zone. This means that this LCW distribution is still proportional to the number of occupied bands for all $\mathbf{k}$. The calculation with the hypothetical flat positron wave function demonstrates that the long-wavelength structure, observed in the integrated LCW distributions of the 2γ momentum distribution with the full positron wave function included, is entirely due to the inhomogeneous distribution of the positron charge in the unit cell.

IV. DISCUSSION

The band-structure calculation by Norman *et al.*[15] and our own calculation agree reasonably well. This is especially satisfying in view of the different descriptions used for the potential in the (large) interstitial region, i.e., the atomic-sphere approximation (ASA) for the LMTO calculation versus our warped muffin-tin approximation. The small dispersion of the energy bands near E_F makes both the Fermi surface and the DOS at E_F very sensitive to small shifts of the bands. The electronic specific-heat coefficient γ as deduced from the DOS is less than 10 mJ/mol K^2; however, values twice as large are obtained when E_F is shifted by a few mRy. Since we performed our calculations without spin polarization, this result has to be compared with the experimental γ value measured in the paramagnetic state, i.e., above the Néel temperature of 17.5 K. As its direct measurement suffers from interference by crystal-field excitations,[18] the value of γ in the paramagnetic state is derived from the value in the antiferromagnetic state.[19] To that end one assumes that the antiferromagnetic order will remove a part of the DOS at E_F such that the paramagnetic value of γ exceeds the antiferromagnetic value of 65 mJ/mol K^2. Although other interpretations of the phase transition at 17 K have been suggested,[19] the enhancement of the calculated γ value appears to be larger than a factor of 4, which gives an indication of the importance of many-body effects in the description of the electronic structure of URu_2Si_2.

Although the influence of the positron wave function on the structure in the LCW-folded distribution after integration is very large, it does not dominate the 2γ momentum distribution itself. The Fermi-surface effects are relatively small owing to the large number of occupied bands;[20] hence, an experimental 2D-ACAR study should first of all focus on the description of the symmetry of the electron wave functions, especially those of the f states. The hybridized f bands have been shown to contribute to the 2γ momentum distribution in a very anisotropic manner. More specifically, a 2D-ACAR measurement with the integration direction along the [001] axis can be expected to display clear anisotropic structure for momenta larger than 1 a.u., which can be attributed to the f states.

The results presented in this paper demonstrate that the computation of the 2γ momentum distribution is essential for an experimental derivation of the Fermi surface of URu_2Si_2 by an LCW analysis of 2D-ACAR data. The inhomogeneous distribution of the positron density in complex systems such as URu_2Si_2 causes only a small $\mathbf{k}$ dependence in the filled-band contributions to the 3D LCW distribution, but, as the wavelength of this variation is of the same size as the Brillouin zone, its effect may be substantially enhanced after integration along certain directions. The broad large maxima at XP in Fig. 8(a) illustrate this most clearly. Fermi-surface sheets, on the other hand, give rise to sharper structure but are often (much) smaller than the Brillouin zone and hence their signature is less enhanced by the integration. One may, however, find directions of integration, like the [101] integration direction in the case of URu_2Si_2, for which one or more individual Fermi-surface sheets stand out without significant interference from other structure. Tomographical reconstruction of the 3D 2γ momentum distribution[1] in principle dispenses with the problems caused by projection, but requires 2D-ACAR data measured under identical conditions for many sample orientations. In the absence of a reliable reconstruction of experimental data, which is unfortunately the case in many 2D-ACAR studies, 2γ momentum distribution calculations constitute an essential guide in the interpretation of the experiment.

The most important result of the present calculations is the observed affinity of the positron for the U site in URu_2Si_2. As this is the result of the large space around the U atom, the same effect is expected to occur in the whole series of UT_2Si_2 and CeT_2Si_2 ternary alloys, with T a transition-metal atom, which have been studied extensively by Palstra.[21] Although it would be a major enterprise, this creates the possibility for a systematic study of the electronic structure of f-electron systems, ranging from Pauli paramagnetism via heavy fermions (URu_2Si_2, $CeCu_2Si_2$, and $CeRu_2Si_2$) to local-moment behavior. As an additional advantage, the partial substitution of the respective components, yielding pseudoternary alloys,[22] does not disturb the observation of the electronic-structure effects by the positron-annihilation technique, contrary to the situation in de Haas—van Alphen experiments. The finite lifetimes of the electron states caused by substitutional disorder can be shown to merely broaden the Fermi-surface discontinuities in the 2γ momentum distribution.[23] The observation of f electrons may not be restricted to the compounds mentioned above. The crystal structures of some other heavy-fermion systems also leave large open volumes for the U or Ce atoms. Tanigawa *et al.*[24] have performed 2D-

ACAR measurements on CeB_6; however, the observed structure in the LCW distributions could not be described satisfactorily by the calculated Fermi surface. This was attributed to positron wave-function effects, but Springford and Reinders[25] have shown that, according to their de Haas–van Alphen experiments, the Ce f electrons hardly contribute to the formation of the Fermi surface. The intermediate-valence compound $CeNi_5$ has been the subject of 2D-ACAR experiments by Jarlborg *et al.*[26] Their results could not be interpreted by a local-density-approximation (LDA) band calculation, a fact ascribed to the localized character of the Ce f electrons. Although the observed effects in both systems are not necessarily caused by the Ce f electrons, their crystal structures, like URu_2Si_2, seem to leave a large volume for the Ce atom and, consequently, may provide a significant overlap of the positron wave function with the f states. Owing to the somewhat more extended nature of the uranium f electrons, U compounds (we mention UBe_{13} here) are preferred to Ce compounds, especially now that the numerical calculation of the relativistic 2γ momentum distribution is possible.[4]

V. CONCLUSIONS

The calculated band structure of URu_2Si_2 displays the flat U f bands at the Fermi level hybridized with conduction electrons originating from ligand atoms, characteristic of a heavy-fermion system. The positron wave function displays a clear affinity for the U atom yielding a relatively large overlap with the f-electron states. The amplitudes of the discontinuities in the 3D LCW-folded 2γ momentum distribution are large considering the localized nature of the f electrons. Consequently, observation of the Fermi surface with the aid of the 2D-ACAR method appears feasible. Integration of the LCW distribution along the [001] direction yields small Fermi-surface effects in addition to large features contributed by the inhomogeneity of the positron wave function. The [101]-integration direction is found to be favorable for the observation of the Fermi surface. However, owing to the large number of occupied bands, the positron-annihilation experiments are expected to yield the most specific information about the symmetry of the wave functions, including the f-electron states.

ACKNOWLEDGMENTS

One of the authors (G.J.R.) gratefully acknowledges the hospitality of Argonne National Laboratory. Discussions with R. Benedek and M. Norman were highly appreciated. The calculations at ECN were facilitated by the assistance of J. Hollenberg, B. van Corler, and M. van Waveren of the Stichting Academisch Rekencentrum, Amsterdam (SARA). The work at ECN was part of the research program of the Stichting Fundamenteel Onderzoek der Materie (Foundation for Fundamental Research on Matter) and was made possible by financial support from the Nederlandse Organisatie voor Wetenschappelijk Onderzoek (Netherlands Organization for the Advancement of Research). The supercomputer time was financed by the "Nationaal Fonds Gebruik Supercomputers (NFS)" via the Foundation SURF. The work at Argonne was supported by the U.S. Department of Energy (Division of Materials Science of the Office of Basic Energy Sciences) under Contract No. W-31-109-ENG-38 and by a grant of computer time on the Cray-2 supercomputer at the National Energy Research Supercomputer Center (Livermore, CA).

[1]S. Berko, in *Positron Solid-State Physics,* edited by W. Brandt and A. Dupasquier (North-Holland, Amsterdam, 1983), p. 64.

[2]P. E. Mijnarends, in *Positron Solid State Physics* (Ref. 1), p. 146.

[3]V. Devanathan and K. Iyakutti, J. Madras Univ. B **45**, 188 (1982).

[4]G. J. Rozing, P. E. Mijnarends, and R. Benedek, Phys. Rev. B **43**, 6996 (1991).

[5]M. B. Maple, J. W. Chen, Y. Dalichaouch, T. Kohara, C. Rossel, M. S. Torikachvili, M. W. McElfresh, and J. D. Thompson, Phys. Rev. Lett. **56**, 185 (1986).

[6]A. de Visser, F. E. Kayzel, A. A. Menovsky, J. J. M. Franse, J. van den Berg, and G. J. Nieuwenhuys, Phys. Rev. B **34**, 8168 (1986).

[7]G. R. Stewart, Rev. Mod. Phys. **56**, 755 (1984).

[8]C. Broholm, J. K. Kjems, W. J. L. Buyers, P. Matthews, T. T. M. Palstra, A. A. Menovsky, and J. A. Mydosh, Phys. Rev. Lett. **58**, 1467 (1987).

[9]G. Aeppli, E. Bucher, A. I. Goldman, G. Shirane, C. Broholm, and J. K. Kjems, J. Magn. Magn. Mater. **76&77**, 385 (1988).

[10]A. J. Arko and D. D. Koelling, Phys. Rev. B **17**, 3104 (1978).

[11]J. J. Dongarra, J. R. Gabriel, D. D. Koelling, and J. H. Wilkinson, J. Comput. Phys. **54**, 278 (1984).

[12]L. Hedin and B. J. Lundqvist, J. Phys. C **4**, 2064 (1971).

[13]D. D. Koelling, Solid State Commun. **53**, 1019 (1985).

[14]The present calculations do not take into account positron electron correlation. Using two-component density-functional theory, Boronski and Nieminen [Phys. Rev. B **34**, 3820 (1986)] have shown that these correlation effects can be included in the form of an extra potential term, which is added to the Hartree-Coulomb potential and acts toward smoothing the inhomogeneous e^+ density. This term varies by less than 0.2 Ry for electron densities between $r_s=2$ and 8 (where $4\pi r_s^3/3$ is the volume per electron) and its inclusion may transfer some positron density from the space between the U atoms to the positions between the U and Si atoms (the interstitial e^+ Hartree potential between the Si atoms is ~ 1 Ry higher than in the two regions just mentioned, and thus remains unfavorable for the e^+). Since this tends to bring the positron closer to the U atoms, it might well increase the overlap between the positron and the U $5f$ electrons and hence be favorable to the observation of f orbital effects. We expect, however, that the results remain qualitatively unchanged.

[15]M. R. Norman, T. Oguchi, and A. J. Freeman, Phys. Rev. B **38**, 11 193 (1988).

[16]D. G. Lock, V. H. C. Crisp, and R. N. West, J. Phys. F **3**, 561 (1973).

[17]See, for instance, L. P. L. M. Rabou and P. E. Mijnarends, Solid State Commun. **52**, 933 (1984).

[18]B. Renker, F. Gompf, E. Gering, P. Frings, H. Rietschel, R. Felten, F. Steglich, and G. Weber, Physica B **148**, 41 (1987).

[19]U. Rauchschwalbe, Physica B **147**, 1 (1987).

[20]Structure in the LCW-folded distributions due to Fermi-surface sheets where the electrons are strongly correlated will be reduced further since correlations act to decrease the step in the momentum density $n(\mathbf{p})$ of the electrons [see S. Doniach, in *Momentum Distributions,* edited by R. N. Silver and P. E. Sokol (Plenum, New York, 1989), p. 235]. This may reduce the already weak f-band breaks beyond experimental resolution.

[21]T. T. M. Palstra, A. A. Menovsky, G. J. Nieuwenhuys, and J. A. Mydosh, J. Magn. Magn. Mater. **54-57**, 435 (1986).

[22]Y. Dalichaouch, M. B. Maple, J. W. Chen, T. Kohara, C. Rossel, M. S. Torikachvili, and A. L. Giorgi, Phys. Rev. B **41**, 1829 (1990).

[23]P. E. Mijnarends, L. P. L. M. Rabou, K. E. H. M. Hanssen, and A. Bansil, Phys. Rev. Lett. **59**, 720 (1987).

[24]S. Tanigawa, T. Kurihara, M. Osawa, T. Komatsubara, and Y. Onuki, in *Positron Annihilation,* edited by L. Dorikens-Vanpraet, M. Dorikens, and D. Segers (World Scientific, Singapore, 1989), p. 239.

[25]M. Springford and P. H. P. Reinders, J. Magn. Magn. Mater. **76&77**, 11 (1988).

[26]T. Jarlborg, A. A. Manuel, M. Peter, D. Sanchez, A. K. Singh, J. L. Stephan, E. Walker, W. Assmuss, and M. Hermann, in *Positron Annihilation* (Ref. 24), p. 266.